Japanese Journal of Veterinary Research 63(1): 25–36, 2015

FULL PAPER

Morphological characteristics observed during early follicular development in perinatal MRL/MpJ mice

Yuma Yamashita[1)], Teppei Nakamura[1, 2)], Saori Otsuka-Kanazawa[1)], Osamu Ichii[1)] and Yasuhiro Kon[1*)]

[1)]Laboratory of Anatomy, Department of Biomedical Sciences, Graduate School of Veterinary Medicine, Hokkaido University, Kita18-Nishi 9, Kita-ku, Sapporo 060–0818, Japan

[2)]Section of Biological Safety Research, Chitose Laboratory, Japan Food Research Laboratories, 2–3, Bunkyo, Chitose 066–0052, Japan

Received for publication, October 16, 2014; accepted, January 5, 2015

Abstract

In perinatal mice, the ovary undergoes drastic morphological changes, as clusters of oocytes called nests break into smaller cysts and subsequently form individual follicles. We studied perinatal oocyte development in MRL/MpJ mice, and compared it to that observed in C57BL/6 mice between embryonic day 18.5 and postnatal day 4. Throughout the observation period, compared to C57BL/6 mice, MRL/MpJ mice displayed significantly fewer oocytes in their ovaries. Morphologically, there were no clear differences between the strains at embryonic day 18.5. However, the beginning of folliculogenesis, as evidenced by the expression of NOBOX oogenesis homeobox (Nobox) transcript and protein, was more enhanced in MRL/MpJ mice than in C57BL/6 mice at embryonic day 18.5 and postnatal day 0. In addition, developed follicles were more frequently observed in MRL/MpJ mice than in C57BL/6 mice between postnatal days 0 and 4. In conclusion, the oocyte development during nest breakdown and folliculogenesis was accelerated in MRL/MpJ mice when compared to that observed in C57BL/6 mice.

Key Words: folliculogenesis, MRL/MpJ, nest breakdown, oocyte

Introduction

Reproductive potential in mammalian females is determined by the establishment of primordial follicle pools at the time of birth. In fetal mice, primordial germ cells migrate toward developing gonads, known as the genital ridge, around embryonic day 10.5 (E10.5) and continue to proliferate by way of mitosis until E13.5[25)]. As a result of incomplete cytokinesis during mitosis

*Corresponding author: Dr. Yasuhiro Kon, DVM., Ph. D., Laboratory of Anatomy, Department of Biomedical Sciences, Graduate School of Veterinary Medicine, Hokkaido University, Kita18-Nishi 9, Kita-ku, Sapporo 060–0818, Japan
Phone/Fax: +81–11–706–5189. E-mail: y-kon@vetmed.hokudai.ac.jp
doi: 10.14943/jjvr.63.1.25

in female gonads, proliferating germ cells are connected by intercellular bridges forming structures containing a cluster of germ cells known as a "nest"[22]. Female germ cells undergo meiosis at E13.5, and the primary oocytes are arrested in the diplotene stage of prophase I at the time of birth until puberty[14]. During the perinatal stages in mice, ovarian cords containing the nests become clearly visible throughout the outer and inner ovarian cortices[18], and the oocytes undergo a process called "nest breakdown," where the nests degenerate into smaller cysts until a few individual oocytes remain. Thereafter, the individual oocytes are surrounded by pre-granulosa cells to form primordial follicles that develop into primary follicles[23]. As the nest breakdown progresses, there is a decrease in the number of oocytes with approximately one- to two-thirds of oocytes undergoing programmed cell death[1,13,21].

Previous research has identified several molecules whose functions are crucial for early follicular development in mice. Interestingly, some of their expression changes according to the oocyte development. For example, DEAD (Asp-Glu-Ala-Asp) box polypeptide 4 (*Ddx4*) is expressed in germ cells from the time of their first appearance to adulthood[27]. In addition, Germ cell-specific nuclear antigen (GENA) protein is detectable in ovarian germ cells at E12, but disappears by postnatal day (P) 5[30]. The expression of testis expressed gene 101 (*Tex101*) is specifically observed in nest-stage oocytes[31]. On the other hand, the expression of NOBOX oogenesis homeobox (*Nobox*) transcripts was first detected in oocytes at E15.5 and its expression continues in oocytes of antral follicles[26,29]. Especially, *Nobox* regulates the transcription of genes required for the transition from primordial to primary follicles[29]. Although the ovaries of *Nobox*-deficient mice displayed nests and primordial follicles at birth, the number of oocytes in these mice was observed to decrease 3 days after birth, without the formation of primary follicles[11,26]. Other genes such as the ones encoding bone morphogenetic protein 15 (*Bmp15*) and growth differentiation factor 9 (*Gdf9*) are also known to play important roles in folliculogenesis. *Bmp15*-deficient female mice demonstrate subfertility, which is associated with decreased ovulation and fertilization rates[35], while *Gdf9*-deficient female mice are infertile owing to the arrest in folliculogenesis beyond the primary one-layer follicle stage[6]. Another factor demonstrated by somatic cells, forkhead box L2 (*Foxl2*), is also essential for folliculogenesis. *Foxl2*-deficient female mice are infertile due to impaired follicular development and granulosa cell differentiation from primordial to primary follicles[28,33].

The MRL/MpJ mouse exhibits autoimmune diseases that resemble human systemic lupus erythematosus and rheumatoid arthritis[7,32]. In addition to the autoimmune phenotypes, the reproductive organs of MRL/MpJ mice showed several unique characteristics, including seminiferous epithelial cycle-specific apoptosis of meiotic spermatocytes[8,10], heat shock resistance of spermatocytes[9], production of oocytes in the testis[19], and ovarian cysts originating from the rete ovarii[12]. In addition, the number of primary follicles and the gene expression of several molecules related to early follicular development, such as *Bmp15*, *Gdf9*, and zona pellucida glycoprotein, were observed to be significantly higher in MRL/MpJ mice than in C57BL/6 mice at P0[17]. These findings prompted us to analyze the morphological features of the gonads of MRL/MpJ mice, particularly that of the perinatal ovary. In this study, we demonstrated that nest breakdown, oocyte development, and folliculogenesis were accelerated in perinatal MRL/MpJ mice compared to C57BL/6 mice.

Materials and Methods

Mouse strains: All experiments were performed in accordance with the "Guidelines for the Care and Use of Laboratory Animals" set by the Graduate

School of Veterinary Medicine, Hokkaido University (approved by the Association for the Assessment and Accreditation of Laboratory Animal Care International). C57BL/6 and MRL/MpJ mice were purchased from Japan SLC (Hamamatsu, Japan). The mice were maintained under specific pathogen-free conditions. Newborn female mice were obtained from each strain through free breeding and were killed at P0, P2, or P4 by detruncation. Timed mating was propagated for embryo collection by housing female and male mice together overnight. The female mice were examined for the presence of a vaginal plug denoting pregnancy at noon the following day, when the embryos were at E0.5 of development. The pregnant female mice were killed by CO_2 inhalation euthanasia. The fetuses were then removed and killed by placing on ice.

Sample preparation for light microscopy analysis: At E18.5, P0, P2, and P4, the ovaries of C57BL/6 and MRL/MpJ mice were removed and fixed overnight using 4% paraformaldehyde at 4°C. The ovarian specimens were subjected to fixation, dehydration, and paraffin embedding. Serial sections of the paraffin-embedded blocks with a thickness of 3 μm were prepared.

Immunofluorescence and immunohistochemistry: GENA and Nobox were the cell markers used to identify the developmental stages of oocytes before and after primordial ovarian follicle formation, respectively. In addition, a germ cell marker, Ddx4, and granulosa cell marker, Foxl2, were used to identify the developmental stages in the follicles. The deparaffinized sections were treated with 10 mM citrate buffer for 20 min at 105°C for antigen retrieval. These were then treated with 0.25% casein for 1 hr at room temperature for blocking. The sections were then incubated overnight with either a combination of rat anti-GENA antibody (1 : 400, clone No. TRA98, BioAcademia, Osaka, Japan) and rabbit anti-Nobox antibody (1 : 200, Abcam, Cambridge, UK), or rabbit anti-Ddx4 antibody (1 : 400, Abcam) and goat anti-Foxl2 antibody (1 : 500, Abcam) at 4°C. The sections were incubated for 1 hr at room temperature with FITC (fluorescein isothiocyanate)-labeled goat anti-rat IgG (immunoglobulin G) (1 : 200, Life Technologies, Carlsbad, CA, USA) and Alexa Fluor-546 labeled donkey anti-rabbit IgG (1 : 500, Life Technologies) for GENA and Nobox double immunofluorescence, and with Alexa Fluor-488 labeled donkey anti-rabbit IgG (1 : 500, Life Technologies) and Alexa Fluor-564 labeled donkey anti-goat IgG (1 : 500, Life Technologies) for Ddx4 and Foxl2 double immunofluorescence. Some sections were counterstained with Hoechst 33342 (1 : 2000, Dojindo, Kumamoto, Japan).

For immunohistochemical staining of Ddx4, deparaffinized sections of E18.5 and P0 ovaries from C57BL/6 and MRL/MpJ mice were treated with 10 mM citrate buffer for 20 min at 105°C for antigen retrieval. These were then incubated in 0.3% H_2O_2/methanol solution for 10 min to quench the endogenous peroxidase activity. The sections were then blocked with 10% normal goat serum (SABPO kit, Nichirei Bioscience, Tokyo, Japan) and were incubated overnight with rabbit anti-Ddx4 antibody (1 : 400, Abcam) at 4°C. The sections were then treated with biotinylated goat anti-rabbit IgG (SABPO kit, Nichirei Bioscience) for 30 min at room temperature. Next, the sections were incubated with streptavidin-peroxidase complex (SABPO kit, Nichirei Bioscience) for 30 min at room temperature. The labeled sections were developed using 3,3'-diaminobenzidine-H_2O_2 solution. Finally, the sections were counterstained with 2.5% phosphotungstic acid and 2.5% aniline blue.

The stained sections were examined under a fluorescence microscope (BZ-9000, Keyence, Osaka, Japan). Histometric analysis was performed using a cross-section containing the ovarian hilus. On the sections double-labeled for GENA and Nobox, the total number of immunopositive cells was counted and was presented as the total number of oocytes. The number of cells positive only for Nobox was also estimated, and the ratio of the

number of Nobox-positive cells to the total number of oocytes was calculated. Further, the area of the ovarian cortex was measured in each section, and the density of immunopositive cells was calculated. To identify the follicle stage, each oocyte with a visible nucleus was categorized into the nest, primordial follicle, primary follicle, or secondary follicle stage. For histometric analyses, 2–4 sections from each side of the ovary (in total, 4–8 sections per mouse) from at least three mice per strain were used, and the average of values obtained for the left and right sides of the ovary was calculated.

Quantitative real-time Polymerase Chain Reaction (qPCR): Total RNA from the left and right whole ovaries of C57BL/6 and MRL/MpJ mice at E18.5, P0, P2, and P4 was extracted using TRIzol reagent (Life Technologies) according to the manufacturer's protocol. Extracted total RNA was treated with DNase (Nippon Gene, Tokyo, Japan), and the complementary DNA (cDNA) was synthesized using ReverTra Ace (Toyobo, Osaka, Japan) and random primers (Promega, WI, USA). qPCR analysis was performed using the Brilliant III SYBR Green QPCR Master Mix on a real-time thermal cycler (MX 3000P; Agilent Technologies, Santa Clara, CA, USA), according to the manufacturer's instructions. The mRNA expression levels of the target genes were normalized against that of actin, beta (*Actb*) or *Ddx4*. The primer pairs used for the experiments are shown in Table 1.

Statistical analysis: For all values, mean ± standard error (SE) was calculated. Mann-Whitney's *U*- test ($P < 0.05$) was used to compare C57BL/6 and MRL/MpJ mice.

Results

Comparison of the ovarian structures of C57BL/6 and MRL/MpJ mice during the perinatal period

At E18.5, several Ddx4-positive oocytes were localized to the ovarian cortices of both C57BL/6 and MRL/MpJ mice. These oocytes were observed to form a cluster, designated as a nest, separated by connective tissues stained blue (Figs. 1A, 1A', 1B, and 1B'). At P0, the nests were still found at the ovarian cortices in both strains (Figs. 1C, 1C', 1D, and 1D'). Some single oocytes, separated from the nest, were observed in the inner ovarian cortices of both C57BL/6 and MRL/MpJ mice; however, these single oocytes were relatively large in MRL/MpJ mice than in C57BL/6 mice (Figs. 1C' and 1D').

Comparison of oocyte development between C57BL/6 and MRL/MpJ mice from E18.5 to P4 stages

During oogenesis, the transit of gene expression in oocyte was observed (Fig. 2A). In order to compare the oocyte development between

Table 1. Sequence of primers used in quantitative PCR reactions

Genes (accession no.)		Primer sequence (5'-3')	Product size (bp)
Ddx4	Forward	TGGGTTTTGGACCAGAGATG	158
(NM_001145885)	Reverse	CCCAACAGCGACAAACAAG	
Tex101	Forward	ATCTTTCTTCTAATCGCCTCACG	121
(NM_019981)	Reverse	GCTCAGCCTTTGAAGTCCAGT	
Nobox	Forward	CATGAAGGGGACCTGAAGAA	153
(NM_130869)	Reverse	GGAAATCTCATGGCGTTTGT	
Actb	Forward	ACTGCTCTGGCTCCTAGCAC	196
(NM007393)	Reverse	CAGCTCAGTAACAGTCCGCC	

Ddx4: DEAD (Asp-Glu-Ala-Asp) box polypeptide 4; *Tex101*: testis expressed gene 101; *Nobox*: NOBOX oogenesis homeobox; *Actb*: actin, beta.

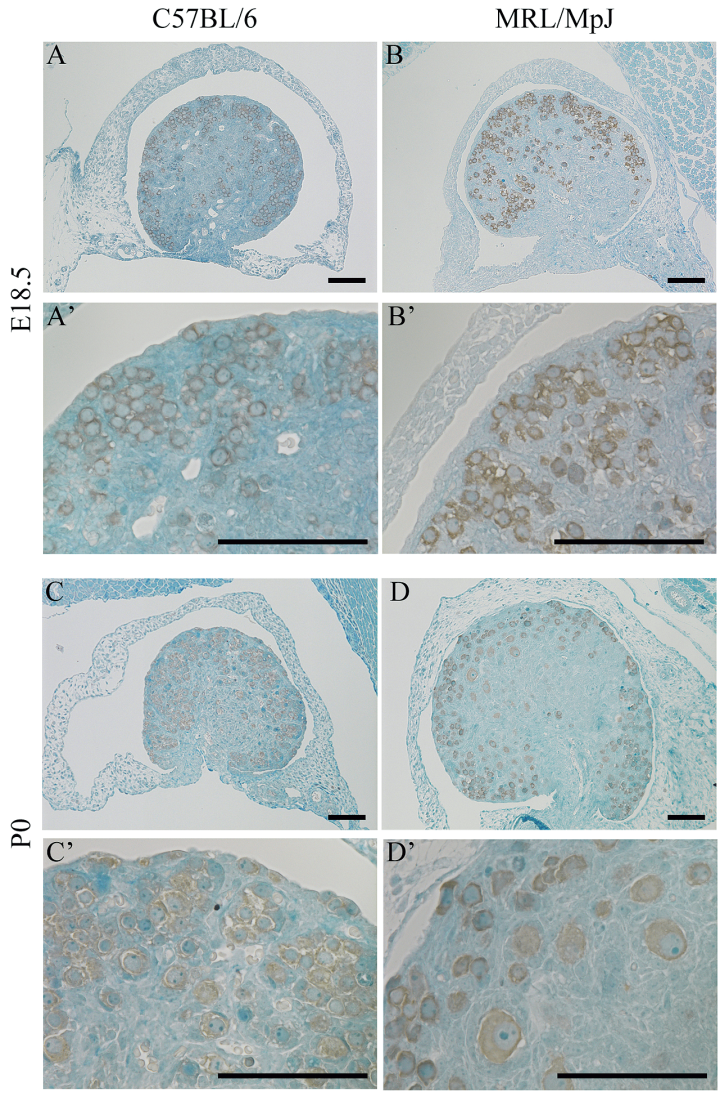

Fig. 1. Ovaries of C57BL/6 and MRL/MpJ mice at E18.5 and P0. The sections were immunostained with a germ cell marker, DEAD (Asp-Glu-Ala-Asp) box polypeptide 4 (Ddx4), and counterstained with 5% phosphotungstic acid and 2.5% aniline blue. **(A and B)** The sections of the ovary at embryonic day 18.5 (E18.5). **(A' and B')** Higher magnification of A and B, respectively. **(C and D)** The sections of the ovary at postnatal day 0 (P0). **(C' and D')** Higher magnification of C and D, respectively. Bars = 100 μm.

C57BL/6 and MRL/MpJ mice, we analyzed the gene expression of oocyte markers, including *Ddx4*, *Tex101*, and *Nobox,* between the E18.5 and P4 stages. The mRNA expression level of *Ddx4* was relatively low in MRL/MpJ mice compared to C57BL/6 mice throughout the observation period, and there was a significant strain-difference at P2 (Fig. 2B). The expression ratio *Tex101*/*Ddx4* was also generally low in MRL/MpJ mice compared to C57BL/6 throughout the observation period, and there was a significant strain-difference at P0 (Fig. 2C). On the other hand, *Nobox*/*Ddx4* mRNA expression in MRL/MpJ mice was relatively higher than in C57BL/6 mice P0 ($P = 0.05$); however, the expression ratio of *Nobox*/*Ddx4* in MRL/MpJ mice became comparable to that of C57BL/6 mice at P2 (Fig. 2D).

We then analyzed the density of oocytes and the transition in GENA and Nobox protein expression in C57BL/6 and MRL/MpJ mice. The localization of GENA- and Nobox-positive cells in the ovaries from E18.5 to P4 stage was examined

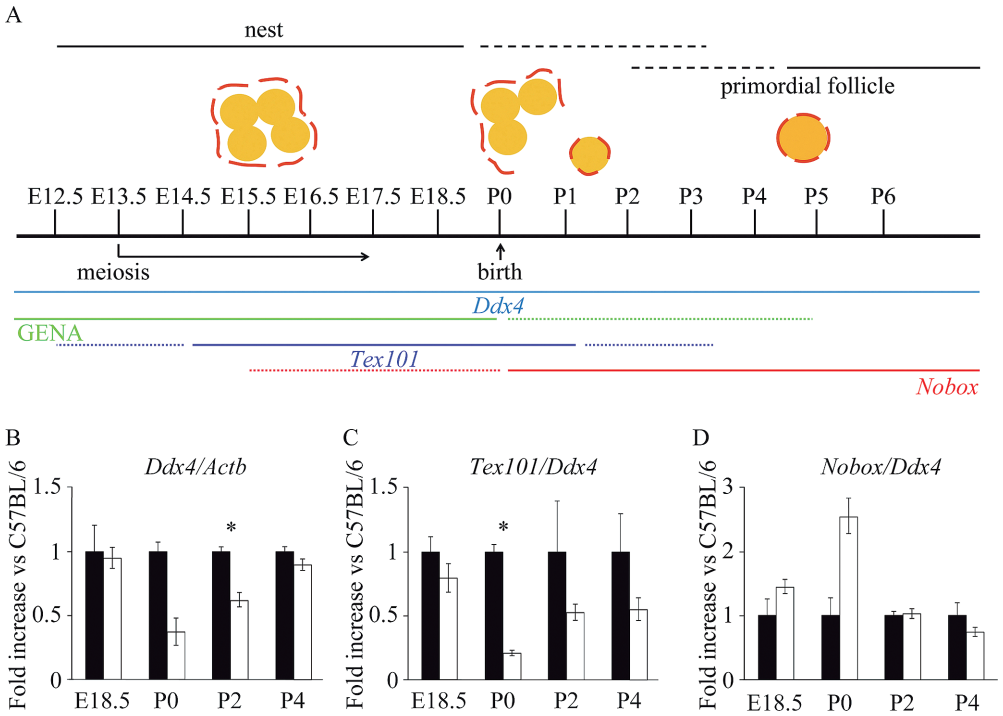

Fig. 2. Oocyte development in mouse ovaries between E18.5 and P4. (A) Time course schema of the expression of the mouse oocyte markers GENA and Nobox. The black lines and scale show the time course of folliculogenesis with respect to the age of the mouse. The illustrations show nest formation, nest breakdown, and primordial follicle formation. The yellow cells represent germ cells, and the dotted line around the germ cells indicates pre-granulosa cells. DEAD (Asp-Glu-Ala-Asp) box polypeptide 4 (*Ddx4*), germ cell-specific nuclear antigen (GENA), testis expressed gene 101 (*Tex101*), and NOBOX oogenesis homeobox (*Nobox*) expression times are indicated by blue, green, purple, and red lines, respectively. The dotted lines indicate weak expression of the corresponding markers. E: embryonic day. P: postnatal day. **(B–D)** Relative expression levels of *Ddx4*, *Tex101*, and *Nobox* in ovaries between C57BL/6 and MRL/MpJ mice. **(B)** The mRNA levels of *Ddx4*. **(C)** The ratio of *Tex101*/*Ddx4* mRNA expression. **(D)** The ratio of *Nobox*/*Ddx4* mRNA expression. Each bar represents the mean ± SE ($n \geq 4$). The Black and white columns indicate C57BL/6 and MRL/MpJ mice, respectively. *: significant difference ($P < 0.05$).

by double immunofluorescence (Figs. 3A–H). As shown in Fig. 2A, GENA and Nobox identified the oocytes before and after the stage of primordial follicle formation, respectively. In both strains, the positive reaction for GENA or Nobox was seen in the nuclei of oocytes at the ovarian cortices (Figs. 3A–H). In C57BL/6 mice, GENA-positive oocytes were abundantly observed in the ovarian cortex at E18.5 (Fig. 3A), and their number decreased with age (Figs. 3A, 3C, 3E, and 3G). On the other hand, several NOBOX-positive oocytes were observed at P0 in the inner position of the ovarian cortex (Fig. 3C), and its numbers increased with age (Figs. 3C, 3E, and 3G) in C57BL/6 mice. Similarly, there were many GENA-positive oocytes observed in MRL/MpJ mice at E18.5, with their numbers decreasing with age (Figs. 3B, 3D, 3F, and 3H). In MRL/MpJ mice, several NOBOX-positive oocytes were observed at E18.5 stage in the inner position of the ovarian cortex. These oocytes were more distinctly observed in MRL/MpJ mice compared to C57BL/6 mice at E18.5 and P0 stages (Figs. 3A–D).

For histoplanimetry, the density of oocytes as quantified by the summed number of GENA-positive and/or Nobox-positive cells in MRL/MpJ mice was significantly lower than that in C57BL/6 mice throughout the observation period (Fig. 3I). In addition, the ratio, in percentage, of the number of Nobox-positive oocytes to the total number of oocytes was significantly higher in

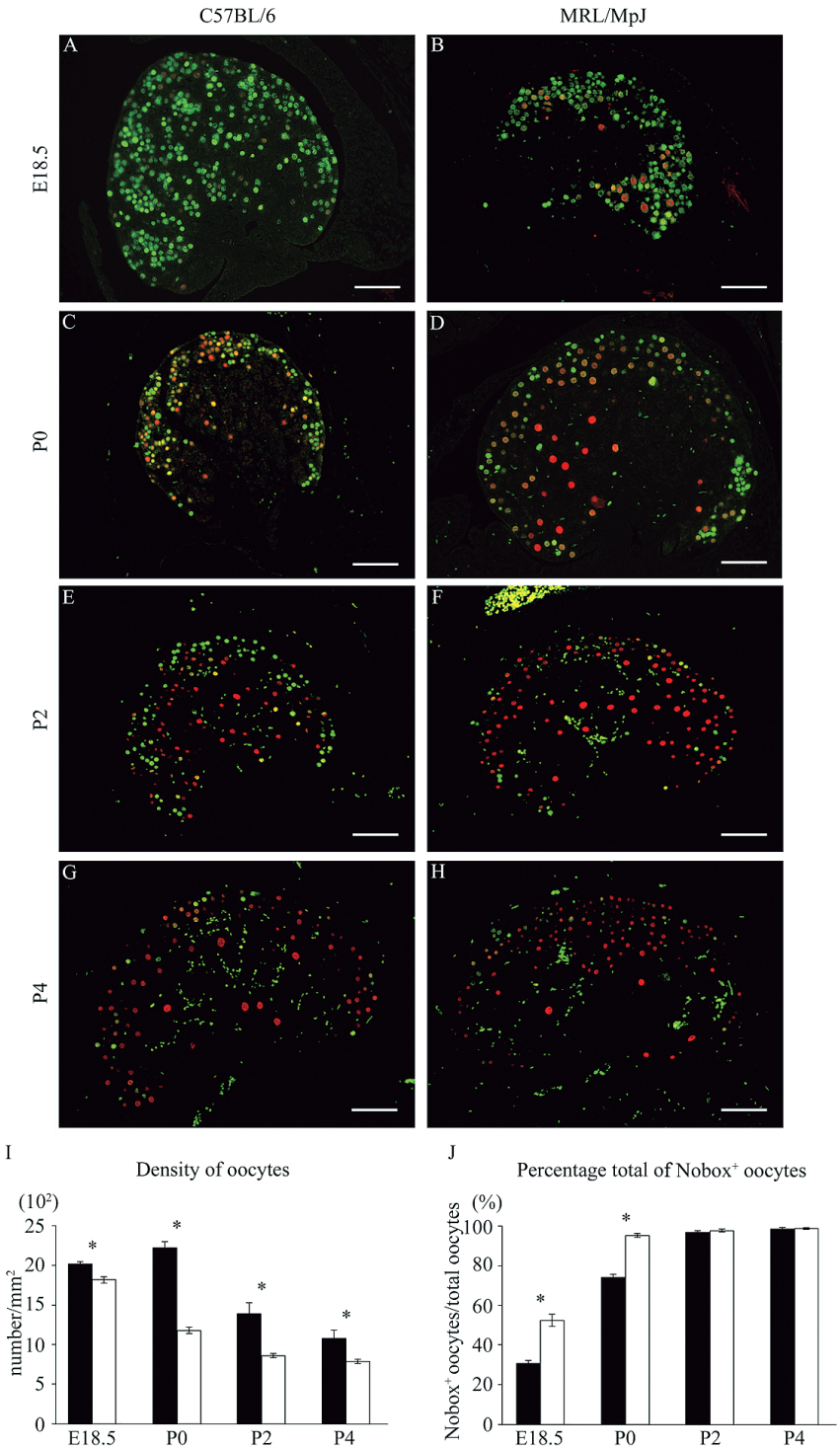

Fig. 3. Immunohistochemical analysis of oocyte development in mouse ovaries between E18.5 and P4. (A–H) Double immunofluorescence staining for germ cell-specific nuclear antigen (GENA) and Nobox in mouse ovaries between the E18.5 and P4 stages. The positive signals for GENA (green) and Nobox (red) are seen in the nuclei of oocytes at the ovarian cortices. Bars = 100 μm. **(I and J)** Quantification of oocytes in mouse ovaries between E18.5 and P4 stages. **(I)** Total number of oocytes as calculated from the total number of immunopositive cells in the merged images of double-labeled (immunofluorescence) sections. **(J)** The ratio of Nobox^{+} oocyte numbers to the total number of oocytes. Each bar represents the mean ± SE ($n \geq 4$). The Black and white columns indicate C57BL/6 and MRL/MpJ mice, respectively. *: significant difference ($P < 0.05$).

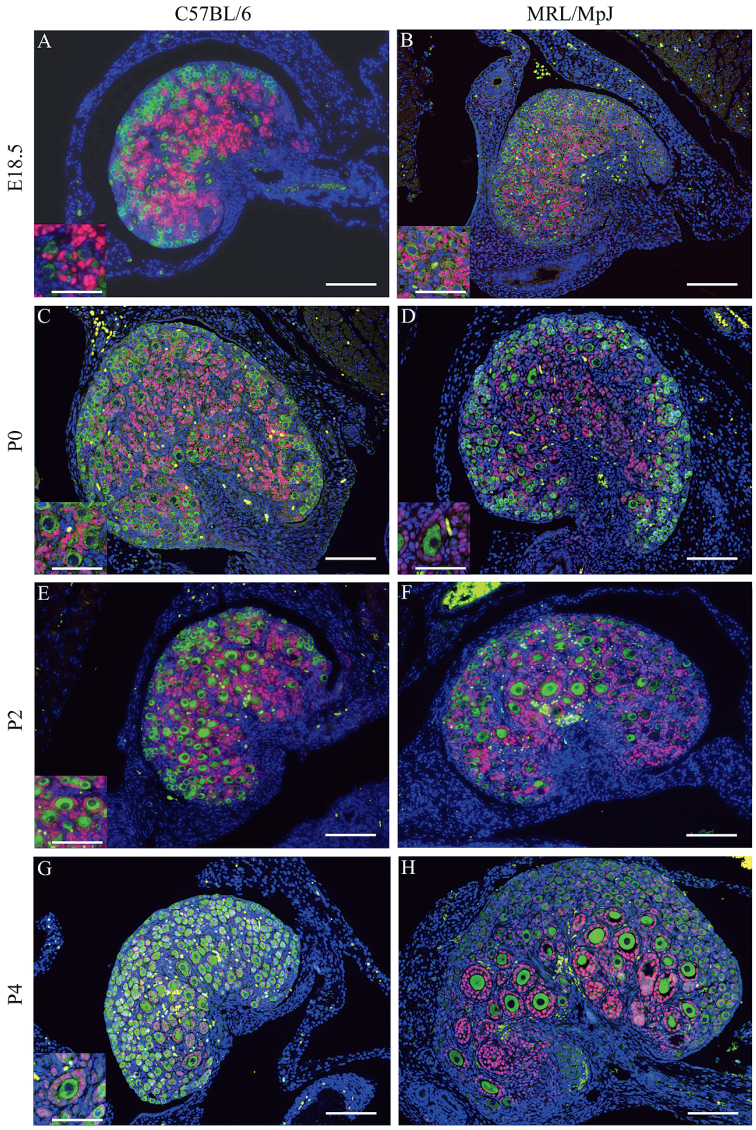

Fig. 4. Follicular development between C57BL/6 and MRL/MpJ mice between E18.5 and P4. (A–H) Double immunofluorescence staining for DEAD (Asp-Glu-Ala-Asp) box polypeptide 4 (Ddx4) and forkhead box L2 (Foxl2) in mouse ovaries between E18.5 and P4 stages. The positive signals for Ddx4 (green) and Foxl2 (red) are detected in the cytoplasm of oocytes and the nuclei of follicular epithelial cells, respectively, in both strains. Nuclei are stained by Hoechst 33342 (blue). Bars = 100 μm (50 μm in insets).

MRL/MpJ mice than in C57BL/6 mice at the E18.5 and P0 stages; however, the values were comparable in both strains at P2 and P4 (Fig. 3J).

Comparison of follicular development between C57BL/6 and MRL/MpJ mice from E18.5 to P4 stages

We compared the follicular stages between C57BL/6 and MRL/MpJ mice using double immunofluorescence of an oocyte marker, Ddx4, and a follicular epithelial cell marker, Foxl2 (Figs. 4A–H). Immunoreactions of Ddx4 and Foxl2 were detected in the cytoplasm of oocytes and nuclei of follicular epithelial cells, respectively, in both strains, throughout the observation period.

At E18.5, numerous Ddx4-positive oocytes were observed within the nest structures in the ovarian cortices of C57BL/6 mice (Fig. 4A). Additionally, a few primordial follicles, which were isolated oocytes surrounded by squamous

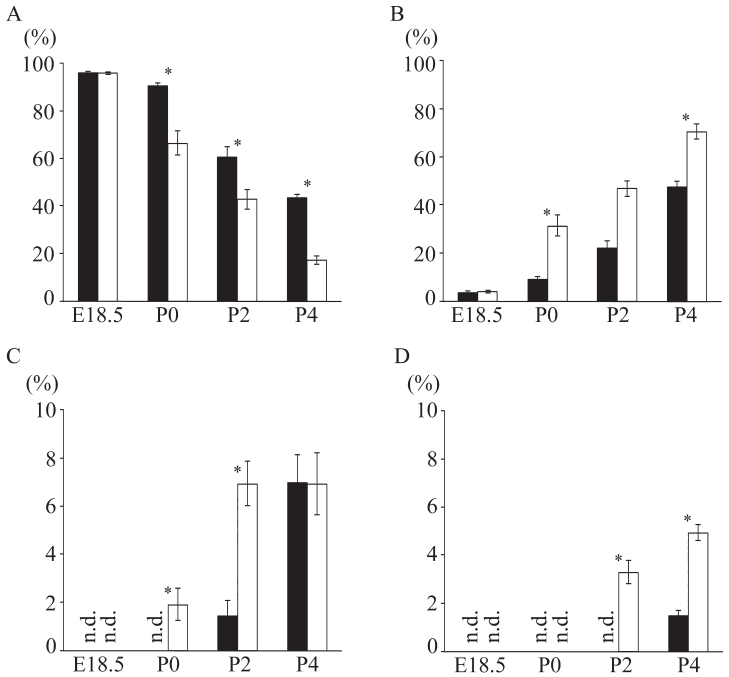

Fig. 5. Quantification of follicular stages in the mouse ovaries between E18.5 and P4. (A) The percentage of oocytes in the nest to total oocytes. **(B)** The percentage of oocytes in the primordial follicles to total oocytes. **(C)** The percentage of oocytes in the primary follicles to total oocytes. **(D)** The percentage of oocytes in the secondary follicles to total oocytes. Each bar represents the mean $\pm$ SE ($n \geq 4$). The Black and white columns indicate C57BL/6 and MRL/MpJ mice, respectively. n.d.: not detected. *: significant difference ($P < 0.05$).

Foxl2-positive follicular epithelial cells, were observed in the inner ovarian cortices of C57BL/6 mice at E18.5 (Fig. 4A, insets), with their number increasing at P0 stage (Fig. 4C). The primary follicles in which oocytes are surrounded by cuboidal follicular epithelial cells, were first detected in the inner ovarian cortices of C57BL/6 mice at P2 (Fig. 4E, inset). At P4, a few primary follicles and secondary follicles (oocytes surrounded by multilayered follicular epithelial cells), were detected (Fig. 4G, inset).

At E18.5, nest structures were observed to be widely spread out in the ovarian cortices in MRL/MpJ mice (Fig. 4B). A few primordial follicles were also observed in the inner ovarian cortices of MRL/MpJ mice at E18.5 (Fig. 4B, inset). Unlike C57BL/6 mice, the primary follicles were first detected in MRL/MpJ mice at P0 (Fig. 4D, inset). At P2, the secondary follicles were detected in the inner cortices of MRL/MpJ mice (Fig. 4F). At P4, the large oocytes contained in primary or secondary follicles were distinctly observed in MRL/MpJ mice (Fig. 4H).

We then examined the percentage of each stage of follicular development. The percentage of oocytes in the nest to total oocytes gradually decreased in C57BL/6 and MRL/MpJ mice during the observation period (Fig. 5A). This percentage was significantly lower in MRL/MpJ mice compared to the C57BL/6 mice at P0, P2, and P4 (Fig. 5A). The percentage of primordial follicles to total follicles gradually increased from E18.5 (Fig. 5B). This percentage was generally higher in MRL/MpJ mice compared to C57BL/6 mice between P0 and P4 stages, and there were significant differences at P0 and P4 (Fig. 5B). The percentage of primary follicles increased after their first appearance at P2 in C57BL/6 mice and at P0 in MRL/MpJ mice (Fig. 5C). This was observed to be significantly higher in MRL/MpJ mice than in C57BL/6 mice at P0 and P2 (Fig. 5C). The secondary follicles were first detected at the P4 stage in C57BL/6 mice and at the P2 stage in MRL/MpJ mice (Fig. 5D). The

percentage of secondary follicles was significantly higher in MRL/MpJ mice than in C57BL/6 mice at P2 and P4 (Fig. 5D).

Discussion

In fetal mouse ovaries, the germ cells form nests within the ovarian cords[18,22]. In perinatal mice, ovaries exhibit drastic morphological changes with the breakdown of the nests in the ovarian cords, and individual oocytes begin to form primordial follicles surrounded by pre-granulosa cells[23]. Since there have been several reports of abnormalities in gonadal morphology and germ cell development related to the genetic background in male MRL/MpJ mice[8–10,17,19–20], we decided to analyze the morphological features of perinatal ovaries in MRL/MpJ mice in this study.

Our research focusing on oocyte development and folliculogenesis in mouse perinatal ovaries between the E18.5 to P4 stages demonstrated large strain-related differences in the degree of progression. The morphology of the ovarian cord was comparable between C57BL/6 and MRL/MpJ mice at E18.5; however, the transitions of expression from *Tex101* to *Nobox* and GENA to Nobox were more advanced in MRL/MpJ mice compared to C57BL/6 mice. At P0, clear structures of ovarian cords containing the nests were preserved in C57BL/6 mice. However, the MRL/MpJ mice showed discontinuous ovarian cords and nest breakdown, as evidenced by the decrease in oocyte numbers within the nests, and the existence of large single Nobox-positive oocytes within the primordial and primary follicles. Nest breakdown and folliculogenesis initiate earlier in the inner ovarian cortices compared to that in the outer cortices have been reported in previous studies[2,3,24].

Although there were no differences in the percentage of Nobox-positive oocytes between C57BL/6 and MRL/MpJ mice at P2, folliculogenesis was still advanced in the MRL/MpJ mice compared to C57BL/6 mice beyond the P0 stage. In addition, the secondary follicles first appeared at P2 in MRL/MpJ mice, while their appearance was first observed at P4 in C57BL/6 mice. These results suggested that the initiation of nest breakdown and folliculogenesis occurred earlier in MRL/MpJ mice than in C57BL/6 mice as previously observed[17]. These differences were also observed to be more pronounced in the inner ovarian cortices compared to the outer ovarian cortices.

Interestingly, the comparison of the density of GENA-positive and Nobox-positive oocyte revealed that the total number of oocytes in the ovary was significantly lower in MRL/MpJ mice than in C57BL/6 mice throughout the observation period. The total number of oocytes was observed to decrease during the P0 stage, and the ratio of the number of Nobox-positive oocytes to the total number of oocytes was higher in MRL/MpJ mice than in C57BL/6 mice. These findings suggest that the transition from GENA-positive oocytes to Nobox-positive oocytes and the resultant loss of oocytes occurred in a more robust manner in MRL/MpJ mice than in C57BL/6 mice. It has been previously reported that the loss of oocytes occurred during nest breakdown through apoptosis or autophagic cell death[4,5,13,21]; therefore, the fewer number of oocytes in MRL/MpJ mice provides additional evidence of accelerated nest breakdown.

We have previously demonstrated stage-specific spermatocyte apoptosis in male MRL/MpJ mice at the pachytene and metaphase stages[8,10,20]. The former is caused by unidentified genes located on chromosome 2[20] and the latter is associated with mutation of exonuclease 1 on chromosome 1[15,16]. In female mice, the oocytes initiate meiosis at E13.5 and reach the pachytene stage by E17.5[34]. Meiosis continues until cells are arrested in the diplotene stage of meiotic prophase I at the time of birth[14]. Metaphase takes place in the oocytes after puberty, just before their ovulation. Therefore, further research is needed to confirm whether the reduced numbers of oocytes found in MRL/MpJ mice have

been a result of accelerated nest breakdown and folliculogenesis and/or the augmented oocyte death controlled by the MRL/MpJ genetic background.

In conclusion, the oocyte development during nest breakdown and folliculogenesis was accelerated in MRL/MpJ mice when compared to that observed in C57BL/6 mice.

Acknowledgements

The research described in this paper was chosen for the Encouragement Award (undergraduate section) at the 156th Japanese Association of Veterinary Anatomists in Iwate (20–22 September 2013). This work was supported by Grant-in-Aid for Scientific Research B (No. 24380156) from the Ministry of Education, Culture, Sports, Science, and Technology, Japan.

References

1) Bristol-Gould, S. K., Kreeger, P. K., Selkirk, C. G., Kilen, S. M., Cook, R. W., Kipp, J. L., Shea, L. D., Mayo, K. E. and Woodruff, T. K. 2006. Postnatal regulation of germ cells by activin: the establishment of the initial follicle pool. *Dev. Biol.*, **298**: 132–148.
2) Byskov, A. G. 1986. Differentiation of the mammalian embryonic gonad. *Physiol. Rev.*, **66**: 71–117.
3) Byskov, A. G., Guoliang, X. and Andersen, C. Y. 1997. The cortex-medulla oocyte growth pattern is organized during fetal life: an in vitro study of the mouse ovary. *Mol. Hum. Reprod.*, **3**: 795–800.
4) Coucouvanis, E. C., Sherwood, S. W., Carswell-Crumpton, C., Spack, E. G. and Jones, P. P. 1993. Evidence that the mechanism of prenatal germ cell death in the mouse is apoptosis. *Exp. Cell Res.*, **209**: 238–247.
5) De Felici, M., Lobascio, A. M., and Klinger, F. G. 2008. Cell death in fetal oocytes: many players for multiple pathways. *Autophagy*, **4**: 240–242.
6) Dong, J., Albertini, D. F., Nishimori, K., Kumar, T. R., Lu, N. and Matzuk, M. M. 1996. Growth differentiation factor-9 is required during early ovarian folliculogenesis. *Nature*, **383**: 531–535.
7) Ichii, O., Konno, A., Sasaki, N., Endoh, D., Hashimoto, Y. and Kon, Y. 2008. Autoimmune glomerulonephritis induced in congenic mouse strain carrying telomeric region of chromosome 1 derived from MRL/MpJ. *Histol. Histopathol.*, **23**: 411–422.
8) Kon, Y. and Endoh, D. 2000. Morphological study of metaphase-specific apoptosis in MRL mouse testis. *Anat. Histol. Embryol.*, **29**: 313–319.
9) Kon, Y. and Endoh, D. 2001. Heat-shock resistance in experimental cryptorchid testis of mice. *Mol. Reprod. Dev.*, **58**: 216–222.
10) Kon, Y., Horikoshi, H. and Endoh, D. 1999. Metaphase-specific cell death in meiotic spermatocytes in mice. *Cell Tissue Res.*, **296**: 359–369.
11) Lechowska, A., Bilinski, S., Choi, Y., Shin, Y., Kloc, M. and Rajkovic, A. 2011. Premature ovarian failure in nobox-deficient mice is caused by defects in somatic cell invasion and germ cell cyst breakdown. *J. Assist. Reprod. Genet.*, **28**: 583–589.
12) Lee, S. H., Ichii, O., Otsuka, S., Hashimoto, Y. and Kon, Y. 2010. Quantitative trait locus analysis of ovarian cysts derived from rete ovarii in MRL/MpJ mice. *Mamm. Genome*, **21**: 162–171.
13) Lobascio, A. M., Klinger, F. G., Scaldaferri, M. L., Farini, D. and De Felici, M. 2007. Analysis of programmed cell death in mouse fetal oocytes. *Reproduction*, **134**: 241–252.
14) McLaren, A. 1984. Meiosis and differentiation of mouse germ cells. *Symp. Soc. Exp. Biol.*, **8**: 7–23.
15) Namiki, Y., Endoh, D. and Kon, Y. 2003. Genetic mutation associated with meiotic metaphase-specific apoptosis in MRL/MpJ mice. *Mol. Reprod. Dev.*, **64**: 179–188.
16) Namiki, Y., Kon, Y., Sasaki, N., Agui, T. and Endoh, D. 2004. Exon skipping of exonuclease 1 in MRL/MpJ mice is caused by a nucleotide substitution of the branchpoint sequence in intron eight. *Jpn. J. Vet. Res.*, **52**: 125–134.
17) Nakamura, T., Otsuka, S., Ichii, O., Sakata, Y., Nagasaki, K., Hashimoto, Y. and Kon, Y. 2013. Relationship between numerous mast cells and early follicular development in neonatal MRL/MpJ mouse ovaries. *PLoS One*, **8**: e77246.
18) Nicholas, C. R., Haston, K. M. and Pera, R. A. 2010. Intact fetal ovarian cord formation promotes mouse oocyte survival and development. *BMC Dev. Biol.*, **10**: 2.

19) Otsuka, S., Konno, A., Hashimoto, Y., Sasaki, N., Endoh, D. and Kon, Y. 2008. Oocytes in newborn MRL mouse testes. *Biol. Reprod.*, **79**: 9–16.
20) Otsuka, S., Namiki, Y., Ichii, O., Hashimoto, Y., Sasaki, N., Endoh, D. and Kon, Y. 2010. Analysis of factors decreasing testis weight in MRL mice. *Mamm. Genome*, **21**: 153–161.
21) Pepling, M. E. 2006. From primordial germ cell to primordial follicle: mammalian female germ cell development. *Genesis*, **44**: 622–632.
22) Pepling, M. E. and Spradling, A. C. 1998. Female mouse germ cells form synchronously dividing cysts. *Development*, **125**: 3323–3328.
23) Pepling, M. E. and Spradling, A. C. 2001. The mouse ovary contains germ cell cysts that undergo programmed breakdown to form follicles. *Dev. Biol.*, **234**: 339–351.
24) Peters, H. 1969. The development of the mouse ovary from birth to maturity. *Acta Endocrinol.*, **62**: 98–116.
25) Peters, H. 1970. Migration of gonocytes into the mammalian gonad and their differentiation. *Philos. Trans. R. Soc. Lond. B Biol. Sci.*, **259**: 91–101.
26) Rajkovic, A., Pangas, S. A., Ballow, D., Suzumori, N. and Matzuk, M. M. 2004. NOBOX deficiency disrupts early folliculogenesis and oocyte-specific gene expression. *Science*, **305**: 1157–1159.
27) Raz, E. 2000. The function and regulation of vasa-like genes in germ-cell development. *Genome Biol.*, **1**: 1017.1–1017.6.
28) Schmidt, D., Ovitt, C. E., Anlag, K., Fehsenfeld, S., Gredsted, L., Treier, A. C. and Treier, M. 2004. The murine winged-helix transcription factor Foxl2 is required for granulosa cell differentiation and ovary maintenance. *Development*, **131**: 933–942.
29) Suzumori, N., Yan, C., Matzuk, M. M. and Rajkovic, A. 2002. Nobox is a homeobox-encoding gene preferentially expressed in primordial and growing oocytes. *Mech. Dev.*, **111**: 137–141.
30) Tanaka, H., Pereira, L. A., Nozaki, M., Tsuchida, J., Sawada, K., Mori, H. and Nishimune, Y. 1997. A germ cell-specific nuclear antigen recognized by a monoclonal antibody raised against mouse testicular germ cells. *Int. J. Androl.*, **20**: 361–366.
31) Takayama, T., Mishima, T., Mori, M., Jin, H., Tsukamoto, H., Takizawa, T., Kinoshita, K., Suzuki, M., Sato, I., Matsubara, S., Araki, Y. and Takizawa, T. 2005. Sexually dimorphic expression of the novel germ cell antigen TEX101 during mouse gonad development. *Biol. Reprod.*, **72**: 1315–1323.
32) Theofilopoulos, A. N. and Dixon, F. J. 1985. Murine models of systemic lupus erythematosus. *Adv. Immunol.*, **37**: 269–390.
33) Uda, M., Ottolenghi, C., Crisponi, L., Garcia, J. E., Deiana, M., Kimber, W., Forabosco, A., Cao, A., Schlessinger, D. and Pilia, G. 2004. Foxl2 disruption causes mouse ovarian failure by pervasive blockage of follicle development. *Hum. Mol. Genet.*, **13**: 1171–1181.
34) Yamaguchi, S., Hong, K., Liu, R., Shen, L., Inoue, A., Diep, D., Zhang, K. and Zhang, Y. 2012. Tet1 controls meiosis by regulating meiotic gene expression. *Nature*, **492**: 443–447.
35) Yan, C., Wang, P., DeMayo, J., DeMayo, F. J., Elvin, J. A., Carino, C., Prasad, S. V., Skinner, S. S., Dunbar, B. S., Dube, J. L., Celeste, A. J. and Matzuk, M. M. 2001. Synergistic roles of bone morphogenetic protein 15 and growth differentiation factor 9 in ovarian function. *Mol. Endocrinol.*, **15**: 854–866.